

# Synthesis of $\gamma$ -Fe<sub>2</sub>O<sub>3</sub>/polypyrrole nanocomposite materials

Kiko Sunderland<sup>a</sup>, Philip Brunetti<sup>a</sup>, Leonard Spinu<sup>a,b</sup>, Jiye Fang<sup>a,c,\*</sup>,  
Zhenjun Wang<sup>b</sup>, Weigang Lu<sup>a</sup>

<sup>a</sup>Advanced Materials Research Institute, University of New Orleans, New Orleans, LA 70148, USA

<sup>b</sup>Department of Physics, University of New Orleans, New Orleans, LA 70148, USA

<sup>c</sup>Department of Chemistry, University of New Orleans, New Orleans, LA 70148, USA

Received 19 January 2004; received in revised form 26 April 2004; accepted 3 May 2004

Available online 4 July 2004

## Abstract

We report a chemical approach for the *in situ* synthesis of conducting polymer-magnetic inorganic nanomaterials with the integration of a high temperature organometallic method and a new microemulsion system containing organic, surfactant and aqueous phases that were established to enable the formation of our host nanocomposite materials. Polypyrrole-based  $\gamma$ -Fe<sub>2</sub>O<sub>3</sub> nanocomposites were prepared through this colloidal system. These organic–inorganic nanocomposites were characterized using X-ray diffraction, transmission electron microscopy, thermogravimetric analysis, electrical resistivity and magnetization measurements. It was observed that the blocking temperature increases with increasing the  $\gamma$ -Fe<sub>2</sub>O<sub>3</sub> nanocomponent in these samples. The resistivity and the temperature variation of resistivity have also been investigated.

© 2004 Elsevier B.V. All rights reserved.

**Keywords:** Nanocomposites; Magnetic materials; Composite materials

## 1. Introduction

The integration of superparamagnetic materials and functional organic materials has attracted an increased interest. Such composite materials exhibit not only super-paramagnetic property but also useful electrical [1] or optical properties [2], offering potential applications in numerous areas such as information storage [3,4], magnetic refrigeration [5,6] and electro-magnetic shields and microwave-absorbing devices [7]. The design and chemical synthesis of paramagnetic-electric nanocomposites are the subjects of our intense current research. Several groups have demonstrated the syntheses of nanometer-sized Fe<sub>3</sub>O<sub>4</sub>-polyaniline [8], Fe<sub>3</sub>O<sub>4</sub>-polypyrrole [1], Fe<sub>3</sub>O<sub>4</sub>-polystyrene [9] and  $\gamma$ -Fe<sub>2</sub>O<sub>3</sub>-polypyrrole [10,11] systems. However, an aqueous processing route at room temperature was commonly used for the fabrication of either Fe<sub>3</sub>O<sub>4</sub> or  $\gamma$ -Fe<sub>2</sub>O<sub>3</sub> inorganic nanoparticles in these reports. In Ref. 11, for example,  $\gamma$ -Fe<sub>2</sub>O<sub>3</sub> nanoparticles as the source of magnetic materials

were synthesized through a room temperature microemulsion method. Notwithstanding these achievements, we realized that it would be more useful if the magnetic properties of these composites could be further enhanced and stabilized. Since the saturation magnetization closely associates to the crystallinity of an inorganic nanocomponent, we replaced this aqueous processing and further employed a high temperature organic solution approach [12–14] to prepare the inorganic nanocrystals with high crystallinity. As demonstrated below, the morphology and crystallinity of  $\gamma$ -Fe<sub>2</sub>O<sub>3</sub> produced in this work are superior to those reported previously.

## 2. Experimental details

The preparation of  $\gamma$ -Fe<sub>2</sub>O<sub>3</sub>/Polypyrrole nanocomposite consists of two stages: pre-synthesis of hydrocarbon-passivated  $\gamma$ -Fe<sub>2</sub>O<sub>3</sub> nanocrystals (NCs) from a high temperature organic solution approach and synthesis of  $\gamma$ -Fe<sub>2</sub>O<sub>3</sub>/Polypyrrole ( $\gamma$ -Fe<sub>2</sub>O<sub>3</sub>/PPY) nanocomposites via an *in-situ* polymerization in oil/water microemulsions. The percentage of the inorganic component was varied by

\* Corresponding author. Tel.: +1-504-280-1057; fax: +1-504-280-3185.

E-mail address: [jfang1@uno.edu](mailto:jfang1@uno.edu) (J. Fang).

adjusting the amount of  $\gamma$ -Fe<sub>2</sub>O<sub>3</sub> NCs in the microemulsion systems.

### 2.1. Preparation of hydrocarbon-passivated $\gamma$ -Fe<sub>2</sub>O<sub>3</sub> NCs

Synthesis of  $\gamma$ -Fe<sub>2</sub>O<sub>3</sub> NCs was conducted through a high temperature processing approach in an organic solution [12] using a setup that is similar to our previous one [13]. A typical experiment is described as follows: under a flowing stream of argon, 1.28 g of oleic acid [CH<sub>3</sub>(CH<sub>2</sub>)<sub>7</sub>CH=CH(CH<sub>2</sub>)<sub>7</sub>CO<sub>2</sub>H, 99+%, ~ 4.56 mmol, Aldrich] and 0.2 ml of iron pentacarbonyl [Fe(CO)<sub>5</sub>, 99.999%, ~ 1.50 mmol, Aldrich] were added into a degassed dioctylether (99%, ~ 18 ml, Aldrich) at 100 °C. The resulting mixture was heated to reflux in a three-neck flask and kept at the refluxing temperature for 1h. The resulting black suspension was cooled to room temperature under argon and 0.57 g of dehydrated trimethylamine N-oxide [CH<sub>3</sub>)<sub>3</sub>NO, 98%, ~ 7.60 mmol, Aldrich] was then added. The mixture was reheated to 130 °C with vigorous stirring under argon for 2 h and subsequently refluxed for an additional 1 h. When the system was cooled to 40 °C, the resulting black precipitate was collected by adding excessive ethanol and centrifugation. The precipitate was re-dispersed into toluene [99.8%, Aldrich] and monodispersed  $\gamma$ -Fe<sub>2</sub>O<sub>3</sub> NCs (designated PY0) were collected after a size-selection post treatment [14] in which a solvent pair containing toluene-ethanol [99.9%, Aldrich] was used.

### 2.2. Synthesis of $\gamma$ -Fe<sub>2</sub>O<sub>3</sub>/PPY nanocomposites

$\gamma$ -Fe<sub>2</sub>O<sub>3</sub>/PPy nanocomposites were synthesized from microemulsion media using an *in-situ* polymerization method. A specific amount of as-prepared  $\gamma$ -Fe<sub>2</sub>O<sub>3</sub> NCs was transferred from toluene into ethyl acetate (CH<sub>3</sub>CO<sub>2</sub>C<sub>2</sub>H<sub>5</sub>, 99.5%, Aldrich) by evaporating the toluene solvent in a vacuum oven and then re-dispersing the NCs into ethyl acetate with an ultrasonication for 1 min. The molar ratio of  $\gamma$ -Fe<sub>2</sub>O<sub>3</sub> to ethyl acetate was varied in each experiment depending on the desired composite ratio in the product. A microemulsion system was established by mixing 15.1 g of SDBS (sodium dodecylbenzenesulfonic acid salt, C<sub>12</sub>H<sub>25</sub>C<sub>6</sub>H<sub>4</sub>SO<sub>3</sub>Na, tech. Grade, Aldrich) as a surfactant, 3.26 g of 1-butanol [CH<sub>3</sub>CH<sub>2</sub>)<sub>3</sub>OH, 99.9%, Aldrich] as a co-surfactant,  $\gamma$ -Fe<sub>2</sub>O<sub>3</sub> NCs in 8.16 g of ethyl acetate as the oil phase and 15.2 mL (0.400 M) of iron (III) chloride (anhydrous FeCl<sub>3</sub>, 98%, Alfa Aesar) solution as the aqueous phase. While stirring vigorously with an overhead stirrer, 0.104 g of freshly distilled pyrrole (98%, Aldrich) was introduced into the system. Polymerization in the microemulsions was completed overnight under agitation at room temperature. In order to remove the residue of the surfactant entirely, the resulting precipitates were rinsed with small amounts of de-ionized water and then washed with acetone, followed by three washes with a mixture of acetone and ethanol (1:2 by volume).

The nanocomposites were recovered by centrifugation and overnight vacuum drying for further characterization. The dried  $\gamma$ -Fe<sub>2</sub>O<sub>3</sub>/PPy nanocomposites (designated PY1, PY2 and PY3) were further doped by dispersion in 1.0 M ammonia solution, washing with de-ionized water and drying under vacuum at least one week before the conductivity measurement.

### 2.3. Characterization

Thermogravimetric analysis (TGA) was conducted using TA Instruments Thermal Analyst 2000 Thermogravimetric Analyzer at a heating rate of 10 °C per min in air from room temperature upto 800 °C. Phase identification was performed at room temperature using an X-ray (CuK<sub>α</sub>) diffractometer (Philips X'pert systems). A JEOL 2010 transmission electron microscope was employed to observe the morphology of the samples. Magnetic characterization was performed with a commercial superconducting quantum interference device (SQUID) magnetometer. Magnetization versus field (−5 T, +5T) and temperature (5K, 350K) were studied for all samples. The magnetization versus temperature curves were measured following the ZFC and FC protocols. The temperature variation of the electrical resistivity for the doped  $\gamma$ -Fe<sub>2</sub>O<sub>3</sub>-polypyrrole nanocomposite samples was measured using a four-point probe method on a Physical Property Measurement System. The samples were cold-pressed in the form of disc pellets with a diameter of 7.3 mm and average thickness of 0.95 mm.

## 3. Results and discussion

The principal procedures in this synthesis involve two steps: preparation of  $\gamma$ -Fe<sub>2</sub>O<sub>3</sub> at high temperature with high crystallinity and introducing these hydrocarbon-passivated  $\gamma$ -Fe<sub>2</sub>O<sub>3</sub> NCs and organic monomers (pyrrole) into the oil nanodroplets of a microemulsion system to carry out an *in-situ* polymerization in these colloidal media. In this work,  $\gamma$ -Fe<sub>2</sub>O<sub>3</sub> NCs have been pre-synthesized according to the standard procedure [12] and characterized. Fig.1(a) shows a TEM image of these  $\gamma$ -Fe<sub>2</sub>O<sub>3</sub> NCs, indicating that these spherical  $\gamma$ -Fe<sub>2</sub>O<sub>3</sub> NCs are about 11–13 nm in size and nearly monodispersed. For a comparison, a TEM image of a sample containing 25.4%wt  $\gamma$ -Fe<sub>2</sub>O<sub>3</sub> NCs and 74.6%wt PPY is also presented in Fig. 1(b), which will be discussed later. As exhibited in the inset of Fig. 2, further XRD characterization demonstrates that they are highly crystalline. Since these as-prepared magnetic NCs are capped with a non-polar organic ligand [12], the passivated hydrocarbons make them redispersible in a non-polar organic phase.

A microemulsion is a thermodynamically stable, isotropic dispersion of oil droplets (5–50 nm in diameter) in a water continuous phase. These colloidal media have been

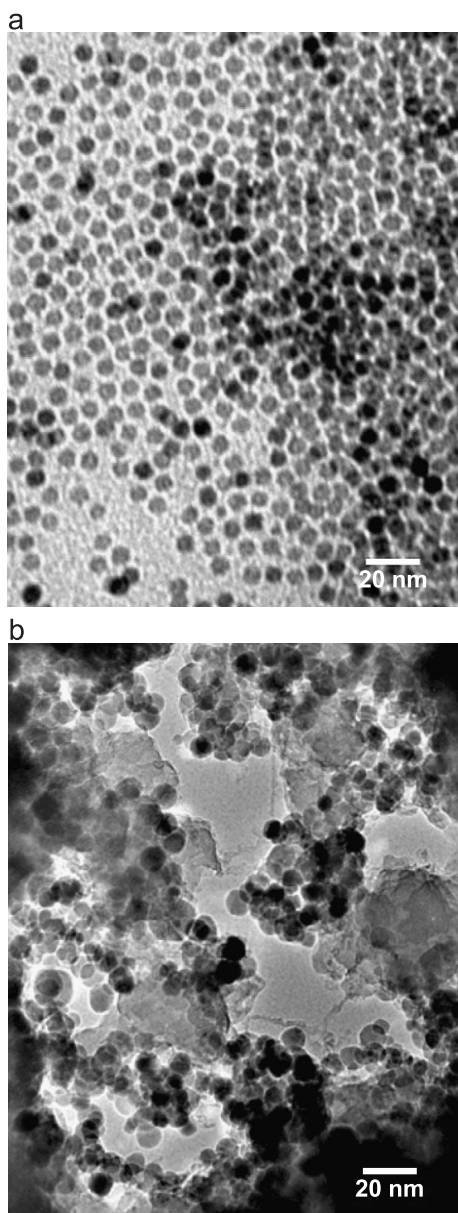


Fig. 1. (a) TEM image of near monodisperse  $\gamma$ - $\text{Fe}_2\text{O}_3$  nanocrystals prepared from a high temperature solution approach. The bar indicates 20 nm. (b) TEM image of  $\gamma$ - $\text{Fe}_2\text{O}_3$ /polypyrrole nanocomposites. The bar indicates 20 nm.

successfully applied to the fabrication of nanometer-sized particles/composites, not only because this approach gives narrow size distribution, but also because it can geometrically control the particle growth, offering a new opportunity for coating the nanoparticles. The oil nanodroplets in microemulsions are stabilized by surfactant molecules (e.g. sodium dodecylbenzenesulfonic acid salt) adsorbed at the oil–water interfaces, acting as “nano-reactors”. Our design is to introduce the magnetic NCs into these “nanoreactors” and to subsequently carry out additional *in-situ* polymerization within these “reactors” as well. Since these “nano-reactors” are surrounded by a surfactant layer (droplet wall), the

growth of as-formed polymers would be efficiently restricted and prevented from further “cross-linking”, possibly forming the “shells” on  $\gamma$ - $\text{Fe}_2\text{O}_3$  NCs. SDBS is a powerful surfactant, and has been widely employed in establishing microemulsion systems, such as the SDBS-toluene-aqueous [15] SDBS-xylene-aqueous [16] systems. It was also reported that the ionic surfactant SDBS can strongly interact with some organic solvents such as pentanol [17] and ethyl acetate [18]. In order to minimize the solubility of as-produced polymer/oligomer in the “oil” phase of microemulsions, we tried to avoid using the aromatic solvent as the “oil” phase. Thus, we selected a microemulsion system reported by X. Yang et al. [11] and initially adopted their recipe to establish our synthetic system containing SDBS/butanol as surfactant/cosurfactant,  $\text{FeCl}_3$  solution as the water phase and ethyl acetate as the oil phase. Unfortunately, we were unable to gain a transparent system and we realized that the nano-droplets might not actually form according to this recipe under our experimental conditions. Therefore, we had to re-map the partial phase diagram for the SDBS/butanol-ethyl acetate-aqueous  $\text{FeCl}_3$  system based on a determination of optical transparency as described elsewhere [19] and we optimized our system points where the multicomponents exist in microemulsion structure. As a result, we determined that the component ratio mentioned in the “experimental details” section is one of the “best” system points.

Fig. 2 shows the TGA curves of various  $\gamma$ - $\text{Fe}_2\text{O}_3$ /polypyrrole nanocomposite samples. It can be seen that all the samples demonstrate three-stage weight loss, a steady weight loss over the temperature range from room temperature to  $\sim 200$  °C and sharp falls in specimen weight over the temperature ranges from  $\sim 250$  to  $\sim 465$  °C and from  $\sim 585$  to  $650$  °C, respectively. The weight loss at

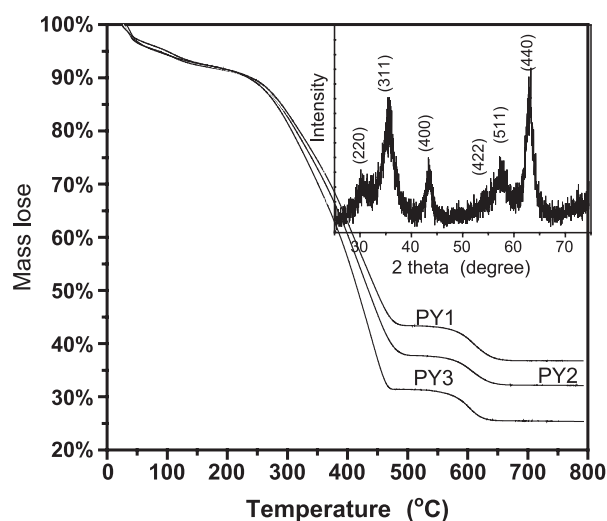


Fig. 2. TGA traces at a heating rate of  $10$  °C/min in argon for various  $\gamma$ - $\text{Fe}_2\text{O}_3$ /polypyrrole nanocomposite samples. Inset: XRD trace of pure  $\gamma$ - $\text{Fe}_2\text{O}_3$  nanocrystals prepared from a high temperature organic solution approach.

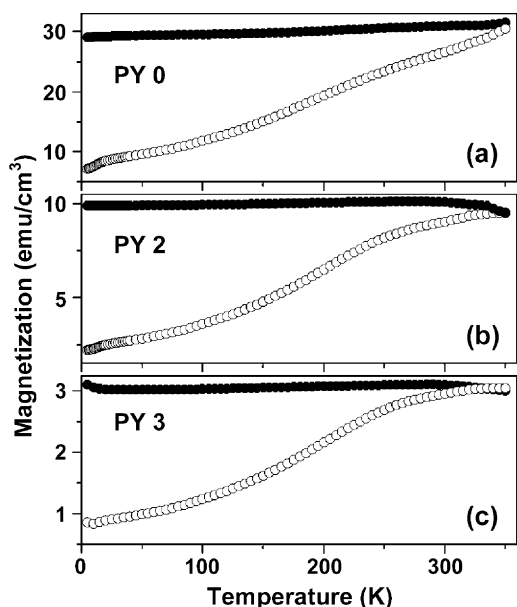


Fig. 3. The ZFC (open symbols) and FC (full symbols) curves for: (a) PY0, (b) PY2 and (c) PY3 samples.

temperatures below 200 °C is due to the elimination of residual organic solvent/monomer in the samples. The fall in specimen weight over the temperature range from ~ 250 to ~ 465 °C is related to the decomposition of polypyrrole as well as the long chain organic capping agent which was capped on the  $\gamma$ -Fe<sub>2</sub>O<sub>3</sub> NCs. The weight loss over the temperature range from ~ 585 to 650 °C can be attributed to the further decomposition of those carbon-containing residues. From the TGA determination, it is estimated that  $\gamma$ -Fe<sub>2</sub>O<sub>3</sub> weight percentages in the three samples are 36.7% (PY1), 32.1% (PY2) and 25.4% (PY3), respectively. We have also examined the homogeneity of the maghemite NCs in polymer by repeating the TG measurements at least once more per sample, obtaining a constant component percentage in each sample determined. As a typical example, Fig. 1(b) demonstrates a TEM image of sample PY3. In comparison with the TEM image of pure  $\gamma$ -Fe<sub>2</sub>O<sub>3</sub> NCs in Fig. 1(a), this image illustrates that the  $\gamma$ -Fe<sub>2</sub>O<sub>3</sub> NCs are present in polypyrrole with considerable homogeneity although it exhibits more disorderly due to the interaction of polymer.

The ZFC (open symbols) and FC (full symbols) curves for samples PY0 (pure  $\gamma$ -Fe<sub>2</sub>O<sub>3</sub> NCs), PY2 and PY3 measured in a field of 100 Oe are shown in Fig. 3. As a general observation we note that the magnetic behavior displayed is typical for fine particle systems where the relaxation of the magnetic moment of the particles is present. In the ZFC process, at the lowest temperatures, the total magnetic moment is nearly zero due to freezing of the moments in random directions. As the temperature is raised, the total magnetic moment increases due to the gradual alignment of moments in the field direction until it reaches the maximum value. In general, the maximum in

the ZFC curve arises due to competition between an increase in the number of particles oriented in the field direction and decrease in the susceptibility of each particle. We note that for our samples we could not observe a very well defined maximum of the ZFC curves in the temperature domain (5K, 350K). However, from the shape of the curves a very clear trend of the variation of the blocking temperature with the concentration of the magnetic nanocrystal in the polymer can be deduced. Thus, as the concentration of the magnetic nanocrystal in the nanocomposite increases the blocking temperature increases. This behavior is consistent with an increase of magnetic dipolar interactions due to the diminishing of average intercrystal distance as the concentration of the magnetic nanocrystal increases [20]. The superparamagnetic behavior of samples PY2 and PY3 at 350 K is confirmed by the zero coercivity observed at this temperature. For sample PY0, the hysteresis loop at 350 K has a coercive field of 10 Oe which indicates that even at this temperature the magnetic behavior of this sample is not fully reversible as in the case of a super-paramagnetism. In Fig. 4, magnetization versus magnetic field curves for PY0 and PY2 samples at 5 K and 350 K are shown. At 5 K all samples present hysteresis with a coercive field of 500 Oe for PY2 and 325 Oe for PY0. One observes that at 350 K the

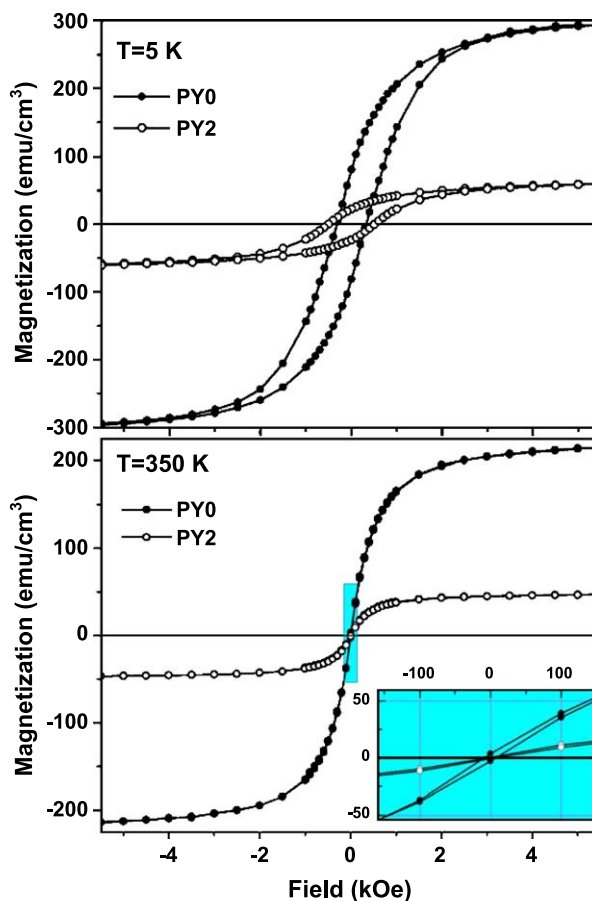


Fig. 4. Magnetization curves for PY0 and PY2 samples at 5 K (top) and at 350 K (bottom). Inset: low field magnetization curves at 350K.

sample PY2 coercive field is zero, which confirms the super-paramagnetic behavior at this temperature predicted by the ZFC and FC curves. Sample PY3, which has a smaller blocking temperature than sample PY2, presents a similar reversible variation of magnetization versus field, with no coercivity at 350 K. For sample PY0, the hysteresis loop at 350 K has a coercive field of 10 Oe (see the inset of Fig. 4) which indicates that even at this temperature the magnetic behavior of this sample is not fully reversible as in the case of superparamagnetism.

At room temperature, the electrical resistivities of all these nanocomposite samples are different, but comparable to that of the pure doped polypyrrole. The higher the polymer concentration in a sample, the lower the resistivity. This is in agreement with the report of  $\gamma$ -Fe<sub>2</sub>O<sub>3</sub>-polyaniline system [21]. It was further observed that as the temperature decreases the resistivity value increases exponentially. Also, it was observed that the temperature variation of resistivity is steeper and is dependent on the polymer content in different samples.

#### 4. Conclusions

$\gamma$ -Fe<sub>2</sub>O<sub>3</sub>-polypyrrole nanocomposites have been synthesized through a combined high temperature organometallic solution and microemulsion–polymerization route. Magnetic characterization shows that the blocking temperature increases with increasing the maghemite nanocomponent. M–H curves measured at 350 K further confirm the super-paramagnetic behavior of these nanocomposite samples. The higher the polymer concentration in a sample, the lower the resistivity. The resistivity of these nanocomposite samples increases exponentially with decreasing the temperature.

#### Acknowledgements

This work was supported by National Science Foundation (EPS-0092001) and Louisiana Board of Regents (NSF/LEQSF(2001-04)-RII-03). Authors thank Dr. Jibao He and

Prof. Jinke Tang for their helps in taking TEM image and in recording XRD pattern, respectively.

#### References

- [1] J. Deng, Y. Peng, C. He, X. Long, P. Li, A.S.C. Chan, *Polym. Int.* 52 (2003) 1182.
- [2] R.F. Ziolo, E.P. Giannelis, B.A. Weinstein, M.P. O'Horo, B.N. Ganguly, V. Mehrotra, M.W. Russell, D.R. Huffman, *Science* 257 (1992) 219.
- [3] L. Gunther, *Phys. World* 3 (1990 December) 28.
- [4] R.G.L. Audran, A.P. Huguenard, U.S. Patent 4,302,523 (1981).
- [5] R.D. McMichael, R.D. Shull, L.J. Swartzendruber, L.H. Bennett, R.E. Watson, *J. Magn. Magn. Mater.* 111 (1992) 29.
- [6] K.A. Gschneidner, V.K. Pecharsky, *J. Appl. Phys.* 85 (1999) 5365.
- [7] P. Gomez-Romero, *Adv. Mater.* 13 (2001) 163.
- [8] M. Wan, W. Zhou, J. Li, *Synthetic Met.* 78 (1996) 27.
- [9] H.-X. Guo, X.-P. Zhao, *Opt. Mater.* 22 (2003) 39.
- [10] M.D. Butterworth, S.A. Bell, S.P. Armes, A.W. Simpson, *J. Colloid Interface Sci.* 183 (1996) 91.
- [11] X. Yang, L. Xu, S.C. Ng, S.O.H. Chan, *Nanotechnology* 14 (2003) 624.
- [12] T. Hyeon, S.S. Lee, J. Park, Y. Chung, H.B. Na, *J. Am. Chem. Soc.* 123 (2001) 12798.
- [13] T. Ji, W.-B. Jian, J. Fang, *J. Am. Chem. Soc.* 125 (2003) 8448.
- [14] J. Fang, K.L. Stokes, W.L. Zhou, W. Wang, J. Lin, *Chem. Commun.* (2001) 1872.
- [15] C. Liu, B. Zou, A.J. Rondinone, Z.J. Zhang, *J. Phys. Chem., B* 104 (2000) 1141; L. Guo, Z. Wu, T. Liu, S. Yang, *Phys. E* 8 (2000) 199; C. Liu, Z.J. Zhang, *Chem. Mater.* 13 (2001) 2092.
- [16] L. Guo, Y. Ji, H. Xu, Z. Wu, P. Simon, *J. Mater. Chem.* 13 (2003) 754.
- [17] R.C. Baker, Th.F. Tadros, in: H.L. Rosano, M. Clausse (Eds.), *Microemulsion Systems*, Marcel Dekker, New York, 1987, pp. 345–356, Section 22.
- [18] K. Matsushita, A.H. Mollah, D.C. Stuckey, C. del Cerro, A.I. Bailey, *Colloids Surf.* 69 (1992) 65.
- [19] J. Fang, N. Shama, L.D. Tung, E.Y. Shin, C.J. O'Connor, K.L. Stokes, G. Caruntu, J.B. Wiley, L. Spinu, J. Tang, *J. Appl. Phys.* 93 (2003) 7483; L.M. Gan, L.H. Zhang, H.S.O. Chan, C.H. Chew, *Mater. Chem. Phys.* 40 (1995) 94.
- [20] J.L. Dormann, L. Spinu, E. Tronc, J.P. Jolivet, F. Lucari, F. D'Orazio, D. Fiorani, *J. Magn. Magn. Mater.* 183 (1998) L255.
- [21] B.Z. Tang, Y. Geng, J.W.Y. Lam, B. Li, X. Jing, X. Wang, F. Wang, A.B. Pakhomov, X.X. Zhang, *Chem. Mater.* 11 (1999) 1581.